Performance of Loran-C 9th Pulse Modulation Techniques

Lee Hartshorn, Peter F. Swaszek, *University of Rhode Island*
Gregory Johnson, Mark Wiggins *Alion Science and Technology*
Richard Hartnett, *U.S. Coast Guard Academy*

BIOGRAPHIES

Lee Hartshorn is a 2002 graduate of the US Coast Guard Academy with a BS in Electrical Engineering. Following graduation he served as an engineer on Coast Guard Cutter BEAR based in Portsmouth, Virginia. After a two-year tour on BEAR, LTJG Hartshorn transferred to the University of Rhode Island, where he is currently pursuing a MSEE.

Peter F. Swaszek is a Professor of Electrical and Computer Engineering at the University of Rhode Island. He received his Ph.D. in Electrical Engineering from Princeton University. His research interests are in digital signal processing with a focus on digital communications and navigation systems. Prof. Swaszek is a member of the Institute of Electrical and Electronics Engineers, the Institute of Navigation, the International Loran Association, , and the American Society of Engineering Education.

Gregory Johnson is a Senior Program Manger at Alion Science & Technology, JJMA Maritime Sector. He heads up the New London, CT office which provides research and engineering support to the Coast Guard Academy and R&D Center. He has a BSEE from the USCG Academy (1987) a MSEE from Northeastern University (1993) and a PhD in Electrical Engineering from the University of Rhode Island (2005). Dr. Johnson is a member of the Institute of Navigation, the International Loran Association, the Institute of Electrical and Electronics Engineers, and the Armed Forces Communications Electronics Association. He is also a Commander in the Coast Guard Reserves.

Richard Hartnett is Head of the Engineering Department at the U.S. Coast Guard Academy (USCGA). He graduated from USCGA with his BSEE in 1977, and earned his MSEE from Purdue in 1980, and his PhD in Electrical Engineering from University of Rhode Island in 1992. He holds the grade of Captain in the U. S. Coast Guard, and has served on USCGA's faculty since 1985. He is the 2004 winner of the International Loran Association Medal of Merit

ABSTRACT

In 2001, the Volpe National Transportation Systems Center completed an evaluation of GPS vulnerabilities and the potential impacts to transportation systems in the United States. One of the recommendations of this study [1] was for the operation of backup system(s) to GPS; Loran-C was identified as one possible backup system. The Federal Aviation Administration (FAA) has been leading a team consisting of members from industry, government, and academia to evaluate the future of Loran-C in the United States with respect to position, navigation, and timing applications (specifically, non-precision approaches for aircraft, harbor approach and entrance for ships, and Stratum 1 frequency and timing). One component of this system development is adding the capability to transmit data messages supporting these applications on the Loran signal itself, frequently called the Loran Data Channel (LDC).

Data transmission on the Loran signal is not a new idea; the Coast Guard experimented with a pulse-position modulated data communication system code named Clarinet Pilgrim in the 1960s. However, the use of advanced DSP-based techniques for receivers, combined with new equipment installations at the U.S. Loran transmitter sites now offers the opportunity for a reliable, higher rate data transmission system. During 2000-2003 a Loran Data Channel that employed phase modulation on 6 of the 8 Loran pulses in a group, called Intrapulse Frequency Modulation (IFM), which achieved a data rate of 250 bps was experimented with. Currently, pulse position modulation of a 9th pulse is being developed. Recently, the Loran Support Unit in Wildwood NJ has been transmitting 9th pulses on their experimental rates. This paper reports on performance evaluation of receiving these test messages at the Coast Guard Academy in New London, CT. Specifically, we look at raw channel symbol error rates (due to cross-rate interference and channel noise) and bit error rates after Reed Solomon decoding.

Report Documentation Page		Form Approved OMB No. 0704-0188

1. REPORT DATE **2006**	2. REPORT TYPE	3. DATES COVERED **00-00-2006 to 00-00-2006**
4. TITLE AND SUBTITLE **Performance of Loran-C 9th Pulse Modulation Techniques**		5a. CONTRACT NUMBER
		5b. GRANT NUMBER
		5c. PROGRAM ELEMENT NUMBER
6. AUTHOR(S)		5d. PROJECT NUMBER
		5e. TASK NUMBER
		5f. WORK UNIT NUMBER
7. PERFORMING ORGANIZATION NAME(S) AND ADDRESS(ES) **U.S. Coast Guard Academy ,31 Mohegan Avenue ,New London ,CT,06320-8103**		8. PERFORMING ORGANIZATION REPORT NUMBER
9. SPONSORING/MONITORING AGENCY NAME(S) AND ADDRESS(ES)		10. SPONSOR/MONITOR'S ACRONYM(S)
		11. SPONSOR/MONITOR'S REPORT NUMBER(S)

12. DISTRIBUTION/AVAILABILITY STATEMENT
Approved for public release; distribution unlimited

13. SUPPLEMENTARY NOTES

14. ABSTRACT

In 2001, the Volpe National Transportation Systems Center completed an evaluation of GPS vulnerabilities and the potential impacts to transportation systems in the United States. One of the recommendations of this study [1] was for the operation of backup system(s) to GPS Loran-C was identified as one possible backup system. The Federal Aviation Administration (FAA) has been leading a team consisting of members from industry government, and academia to evaluate the future of Loran-C in the United States with respect to position navigation, and timing applications (specifically, nonprecision approaches for aircraft, harbor approach and entrance for ships, and Stratum 1 frequency and timing). One component of this system development is adding the capability to transmit data messages supporting these applications on the Loran signal itself, frequently called the Loran Data Channel (LDC). Data transmission on the Loran signal is not a new idea the Coast Guard experimented with a pulse-position modulated data communication system code named Clarinet Pilgrim in the 1960s. However, the use of advanced DSP-based techniques for receivers, combined with new equipment installations at the U.S. Loran transmitter sites now offers the opportunity for a reliable higher rate data transmission system. During 2000-2003 a Loran Data Channel that employed phase modulation on 6 of the 8 Loran pulses in a group, called Intrapulse Frequency Modulation (IFM), which achieved a data rate of 250 bps was experimented with. Currently, pulse position modulation of a 9th pulse is being developed. Recently, the Loran Support Unit in Wildwood NJ has been transmitting 9th pulses on their experimental rates. This paper reports on performance evaluation of receiving these test messages at the Coast Guard Academy in New London, CT. Specifically, we look at raw channel symbol error rates (due to cross-rate interference and channel noise) and bit error rates after Reed Solomon decoding.

15. SUBJECT TERMS

| 16. SECURITY CLASSIFICATION OF:			17. LIMITATION OF ABSTRACT	18. NUMBER OF PAGES	19a. NAME OF RESPONSIBLE PERSON
a. REPORT **unclassified**	b. ABSTRACT **unclassified**	c. THIS PAGE **unclassified**	**Same as Report (SAR)**	**12**	

TRADITIONAL LORAN-C

Loran-C (Long Range Navigation) is a radionavigation system which uses a pulsed transmission at 100 kHz. Extensive details of the Loran system can be found in [2] but the basics are explained here.

Based on the time of arrival of multiple signals from known transmitters, a user's position can be calculated. Figure 1 shows the pulse pattern for the master and three secondary stations in a chain. Each vertical line represents a Loran pulse.
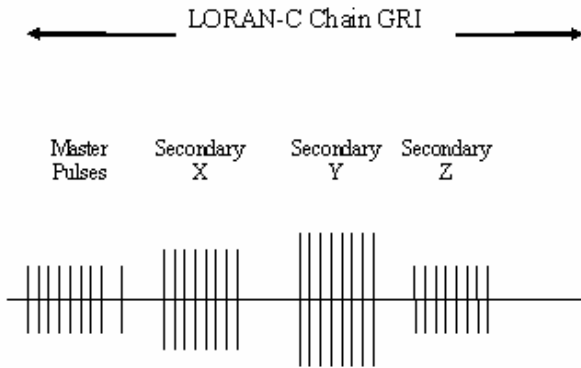
**Figure 1: Loran-C Chain, Station Transmission Timing.**

A master station transmits nine pulses and each secondary station transmits eight pulses. The start of the pulses are spaced 1000 microseconds apart in time, except for the ninth pulse on the master which is spaced 2000 microseconds from the eighth pulse. Each group's pulses (nine for the master and eight for secondary stations) repeat every group repetition interval (GRI). The GRI is the length of time in microseconds between the start of one transmission of master in a Loran-C chain to the start of the next. The GRI designator is used to identify the Loran chain and is the GRI of the chain with the last zero omitted. For example, the Loran chain with a GRI of 99,600 μsec is designated 9960. Figure 2 shows groups of eight pulses from the 9960 chain.
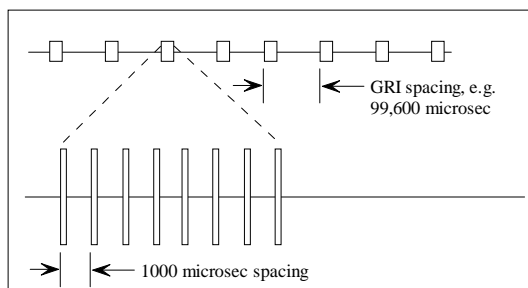

Figure 2: 9960 chain pulse spacing.

Loran towers within a chain transmit sequentially starting with the master station. Each station is labeled sequentially starting with X, then Y, then Z. The time delay until the first secondary station transmits is termed "Emission Delay (ED)," and is chosen such that a user will always receive the master signal before receiving the X-ray secondary, and so forth. Figure 3 shows the emission delay for the X-ray secondary.
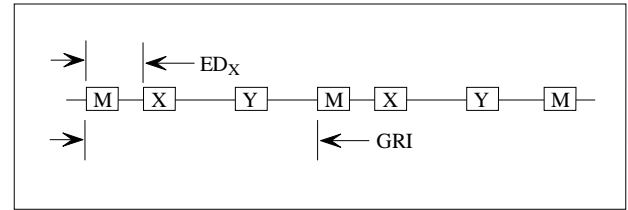

Figure 3: Loran chain Emission Delay.

The pulses are also uniquely phase coded. Figure 4 shows the phase coding, which is repeated every other GRI. Because of the phase coding, the Loran sequence repeats every Phase Code Interval (PCI) or two GRIs.
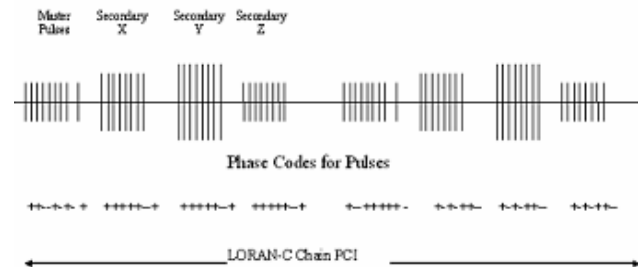

Figure 4: Loran Phase Coding.

The Loran-C pulse shape is shown in Figure 5. The pulse rises from zero to maximum amplitude in 65 μsec and then decays over a 200-300 μsec interval. The pulse shape is designed so that 99% of the radiated power is within the allocated frequency band of 90 to 110 kHz. The third positive cycle zero crossing occurs 30 μsec into the pulse and is called the 'standard zero crossing' and is used as the tracking point.
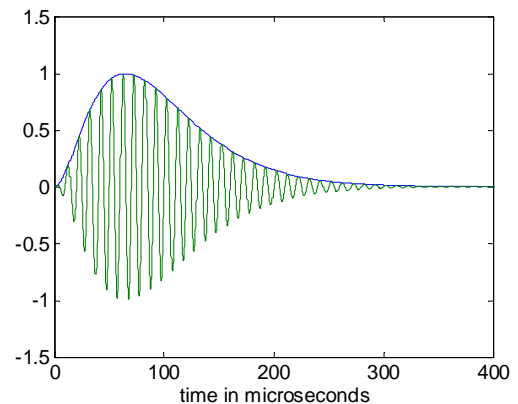
Figure 5: Loran Pulse Shape.

GRIs are chosen to minimize time overlaps between stations from different chains; however, these occurrences cannot be eliminated and are a primary source of error when using Loran for navigation or as a communications channel. This is termed cross-rate interference. Additionally, some stations are dual-rated and transmit on more than one rate which increases the occurrence of cross-rate interference. Other sources of error include channel/receiver noise, and skywave interference. A typical sample of Loran data is shown in Figure 6, highlighting some of the points made throughout this section.
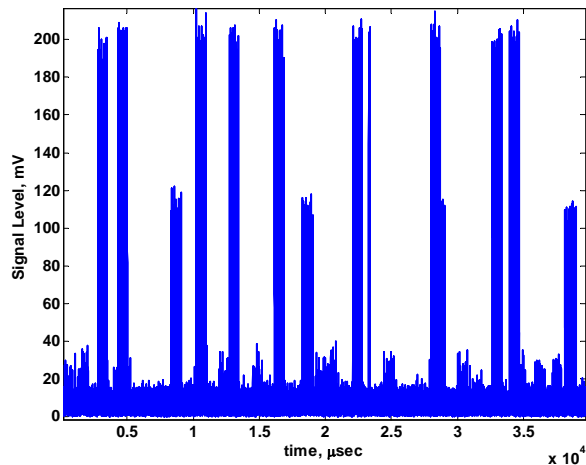
Figure 6: One Second Sample of Loran Data, (magnitude only).

LORAN DATA CHANNEL - BACKGROUND

In order for Loran to become a viable backup to GPS it must provide corrective and system information to users. Modulating data over Loran is not a new concept, but when considering options various aspects of the "navigation" pulses must be considered. Specifically, the Loran-C pulse has many timing and energy specifications that cannot be altered by the data modulation. The Coast Guard experimented with modulation over Loran in the 1960's under a program known as Clarinet Pilgrim [3]. This scheme utilized a binary pulse position modulation (PPM) scheme which shifted the Loran pulse ±1 microsecond. The program proved inefficient with a transfer rate of only a few bits per second (bps).

Following Clarinet, researchers at Delft University of Technology developed an integrated radio navigation and data communication system for Loran-C in the 1990's. The new system, called Eurofix [4], utilizes a ternary scheme which shifts 6 of the 8 Loran pulses in a group by 0 or ±1 microseconds in a balanced pattern. After considerable rate allocation to error correction coding, the resulting data rate is about 30 bps, comparable to the United States' DGPS system. European Loran-C transmitters currently operate employing Eurofix.

In the early 2000's an alternate method of transmitting data by introducing frequency/phase modulation onto 6 of the 8 pulses was considered [5-8]. Called Intrapulse Frequency Modulation (IFM), this method employed a set of 16 pulse waveforms with the modulation occurring after the 30 μsec point so as to have minimal effect on navigation performance. In testing, this system was seen to achieve 250 bps of data rate.

The primary issue with all of these prior modulation methods was their impact on legacy receivers. While balancing the pulse position modulation approaches helped, it did not totally eliminate the additional jitter in the time of arrival (TOA) of signals added by the data modulation. This, in turn, creates errors in determining user position, the primary function of the system. Additionally, the advance and delay of pulses caused an overall reduction of average signal power. From a navigation standing, this was an undesired side affect. Finally, the ability of the Loran transmitters to meet the requirements of these modulation methods was questioned.

Alternatively, the addition of non-navigation pulses was considered to minimize effects on Loran's primary function. Although interleaving pulses between the existing ones was considered, again the question of transmitter capability was an issue. Therefore, system designers settled on the addition of a 9th pulse following the eight navigation pulses in a group. This system is currently in operation on various Loran transmitters in the U.S., and is shown below in Figure 7.
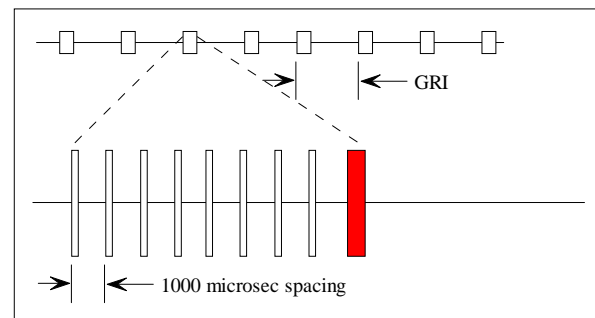

Figure 7: Loran with added 9th Pulse.

## LORAN DATA CHANNEL – 9TH PULSE TECHNIQUES

TIME DOMAIN

Today's 9th Pulse technique of transmitting data is a 32-ary PPM scheme. Each signal choice is defined by a 5 bit symbol such that the first 2 bits specify the coarse delay, and the last 3 specify the finer delay. Figure 8 shows all 32 symbols, pointing out the course delay groups. The complete specification is contained in [9].

Additional Delay: 0   50.625   101.25   151.875
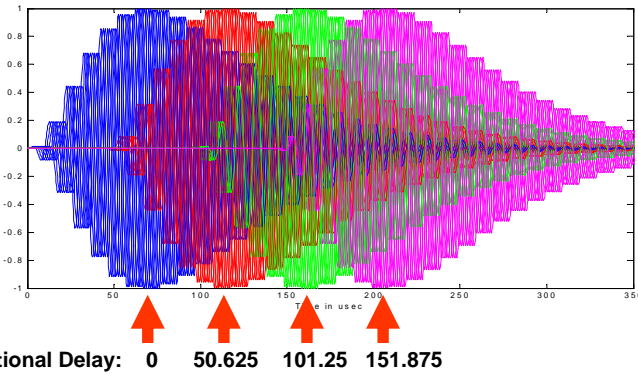
Figure 8: 9th Pulse Modulation.
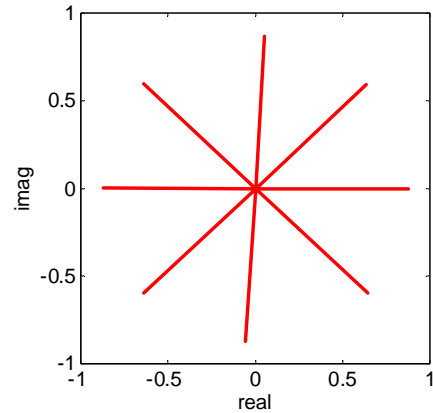
SIGNAL SPACE

Using signal space techniques we can represent each of the above symbols by an N-dimensional vector, where N is the number of orthonormal basis functions needed for a unique geometric representation of the set. While the signals within a single coarse delay groups portray many of the characteristics of phase shift keying, the shifting of the envelope causes the full constellation representing these signals to be 32-dimensional. As all of the signals have equal energy, they can be represented as points on a 32-dimensional hypersphere. Because this is nearly impossible to display graphically, it is easier to look at a single course grouping of eight symbols and extend the concept to the other groups. In signal-space each of these groups resembles 8-PSK (phase shift keying), where the separation between any two signals is ideally 45 degrees. This representation is shown below in Figure 9. Examination of adjacent coarse groups shows an additional 22.5 degrees in phase (approximately) from coarse group to coarse group.
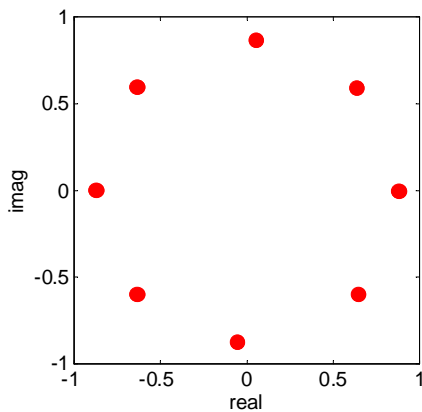
Figure 9: Signal Constellation for 8-PSK.

Since these 8 Loran 9th pulse signals are not exactly PSK, it is instructive to examine their lowpass equivalent signals (on the complex plane). Since a time delay for the bandpass signal corresponds to a phase shift in the lowpass equivalent, then each 9th pulse has the Loran

envelope at a different angle. On a complex plane, these 8 signals take on the form shown in Figure 10; each signal starts at zero, traverses one of the lines emanating out from the origin out to maximum magnitude, and then traverses back to the origin. The particular angle depends upon the amount of delay. Of course, Figure 10 is based upon the idealized model of the 9th pulse signals; we examine actual signals on the complex plane below.

Figure 10: Lowpass equivalent signals on the complex plane (one coarse group).

From a signal space perspective, probability of symbol error performance can be bounded (by the union bound) using the distances to nearest neighbors of each transmitted signal. A closer examination of the distances for the 32-ary PPM 9th pulse scheme shows that each signal is most affected by four or six nearby signals (four for signals in the first and fourth coarse delay groups, six for signals in the middle two delay groups). The relative positions of these signals are:

- two in the same coarse delay group, those with carrier phase difference of ~±45° (equivalently, a delay of ~1.25 μsec) from the desired signal

- two from the prior coarse delay group with carrier phase difference of ~±22.5°

- two from the following coarse group with phase difference of ~±22.5°

(the phase differences are approximate since the actual fine time delays specified for the 9th pulse system are not exactly 1.25 μsec, but are set to match a 5 MHz clock signal). A topologically correct representation of these signals appears in Figure 11.
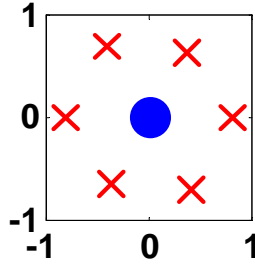
Figure 11: Six Closest Signals.

As is typically the case for high dimension signal sets, it is impractical to exactly calculate the probability of symbol error using the 32 dimension representation; the usual approach is to upper bound the error probability using the union bound. Assuming that the channel noise can be modeled by additive white Gaussian noise (AWGN), the probability of error can be calculated as

$$P_e \leq \frac{1}{32} \sum_{k=1}^{32} \sum_{j \neq i} Q\left(d_{k.j} \sqrt{\frac{\gamma}{2}} \right)$$

Where γ is the SNR and each $d_{k,j}$ is the distance between the kth and j^{th} signals.

It is important to note that this probability of error expression decreases quickly as the SNR increases. Additionally, when demodulating LDC, a receiver would naturally utilize that Loran tower with the highest available SNR. Therefore, to assess system performance, it makes sense to examine typical SNR levels throughout the envisioned coverage area. Figure 12 shows, for each location in the continental US, the expected SNR of the strongest Loran signal present. These expected Loran signal strengths were predicted using the BALOR software at the existing transmitter strengths and are compared to the 50dBμw worst case level of noise nationwide [3] to estimate the SNR. As expected, the highest SNR levels are seen at the locations of the Loran towers, with a decrease with increasing distance from the towers. Worst case performance can be estimated at about 18 dB SNR; in the vast majority of CONUS, the SNR is above about 22 dB.

Utilizing the union bound given above, the probability of error can be computed as a function of SNR and is displayed in Figure 13. At 22 dB SNR, raw 9th pulse symbol error rates of approximately 10^{-5} or better are expected. If channel noise was the single contributing factor to symbol errors it is obvious that we have an extremely robust system with very low error probabilities. However, as mentioned earlier, Loran is also affected by cross rate interference.
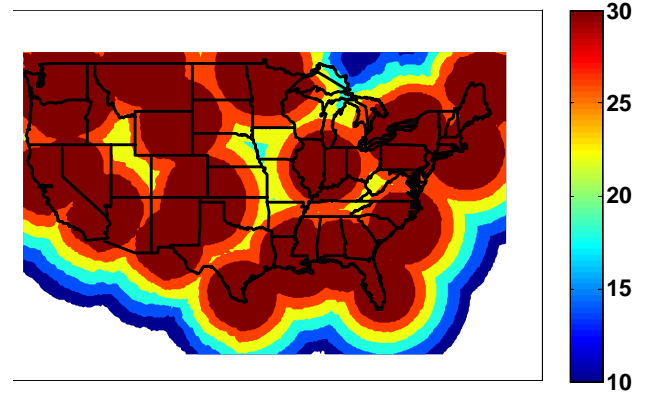

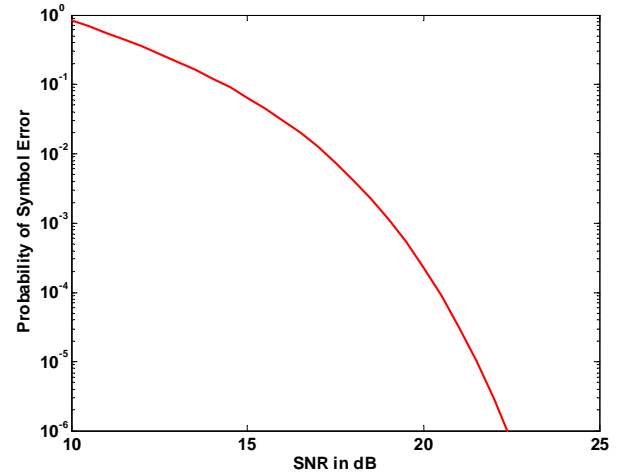**Figure 12: Estimate of the SNR of the strongest Loran signal.**

**Figure 13: Probability of error as a function of SNR.**

CROSS RATE INTERFERENCE - THEORY

In theory, the percentage of pulses that are subject to cross rate interference (CRI) can be calculated. After all, Loran is precisely timed, and each rate repeats indefinitely, creating a periodic occurrence of CRI. To assess the impact of CRI on the 9th pulses, we implemented a "simulation" of the time of occurrences of Loran signal events. We call this a simulation in that it is specific to a particular location at a particular time; however, we expect that the results would be statistically similar at other locations and at other times.

In our algorithm we model each interfering station as periodically generating rectangular pulses or windows in time (with duration of approx 8500 μsec for a secondary, 10,500 μsec for a master), one for each group. Likewise, each 9th pulse occurrence can be modeled by a much shorter duration window (perhaps 300-400μsec) repeating at a different period. (Further, the initial windows are separated in time to model the actual emission delay and propagation delays present.) Advancing these windows at

the respective rates (GRIs) of each station, we look for overlap of the windows. If an overlap occurs, we more closely look to see if the 9th pulse window overlaps with one of the 8 pulses within the larger window; declaring a "hit" if it does. We repeat this operation for additional 9th pulses, until the starting scenario repeats (the number of 9th pulses is the least common multiple of the two rates). Our estimate of cross rate, then, is the percentage of 9th pulses hit. Using this method, which is understandably a worst case estimate of cross rate since even a minimal amount of overlap is counted, we generated the percentages for the different rates and numbers of interfering stations shown in Figure 14. For this figure, the 9th pulse rate is 9960 (LSU) and we examined the hit percentages for the rates normally observed at the US Coast Guard Academy. At first glance, this chart is disturbing; it suggests that many if not most of the 9th pulses will be hit; in reality, the number of interferers observable is usually small and their relative power levels, as seen next, diminish their impact.
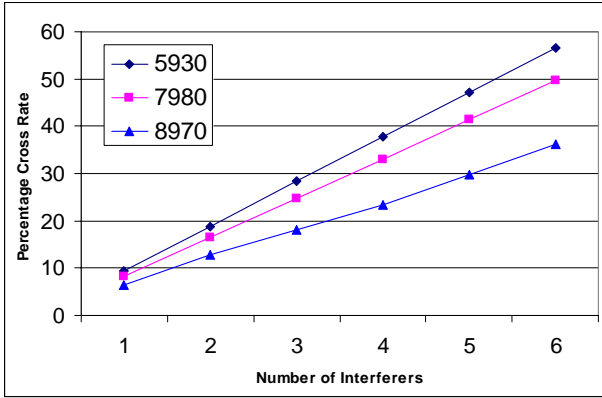

Figure 14: Percentage of cross rate interference hits for the 9960 9th pulses.

Theoretically, the worst case for any cross rate hit coming from a station of SNR less than or equal to that of the 9th pulse of interest is for the crossing signal to appear to be a replica of a different 9th pulse symbol (in other words, perfectly timed and phase with another possible 9th pulse). In this case, the probability of symbol error depends upon the amplitude of the interferer, α, and the minimum distance between the 9th pulse signals, d_{min}, and can be bounded by

$$P_{e,CRI} \leq P_{e,noCRI} + Q\left((1-\alpha)d_{min}\sqrt{\frac{\gamma}{2}}\right)$$

in which the first term, the error probability with no CRI, is as found above. In other words, the CRI can be thought of as an additive effect, decreasing for weaker interferers (as α gets small). In Figure 15 we examine this impact as a function of the signal strength difference of the interfering and 9th pulse signals (the different blue curves)

versus SNR of the 9th pulse signal. As expected, the greatest total probability of error occurs when the interfering signal and data signal have the same SNR, a difference of 0 dB. Once the interferer is more than 15dB weaker than the 9th pulses, the performance is essentially the same as shown in Figure 13 (repeated here in red).
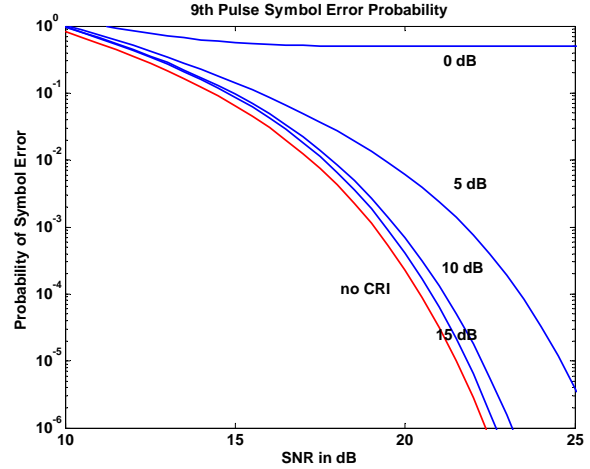

Figure 15: Probability of 9th pulse error versus SNR for various levels of CRI relative to the 9th pulses.

As the impact of cross rate is strongly dependent upon the relative strength of the 9th pulses to each interferer, we return to the BALOR software estimates of Loran signal power nationwide. Figure 16 through Figure 19 show the estimated signal strength differences between the strongest signal and the next four interfering stations, respectively (since most Loran towers are dual rated, we assume that they are all potential interferes to the 9th pulse signal). As you might expect, the greatest difference is at the transmitters, and decreases as you move away from a transmitter.
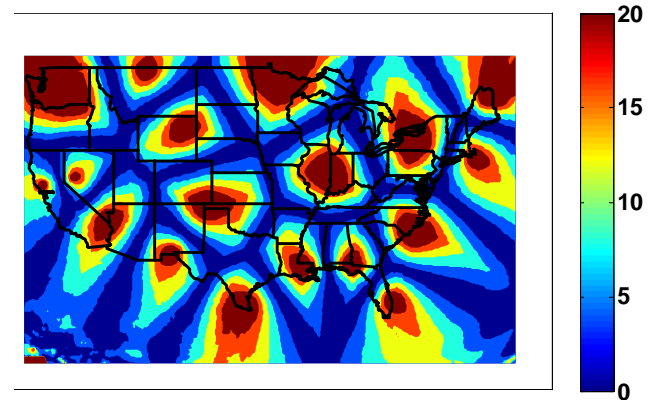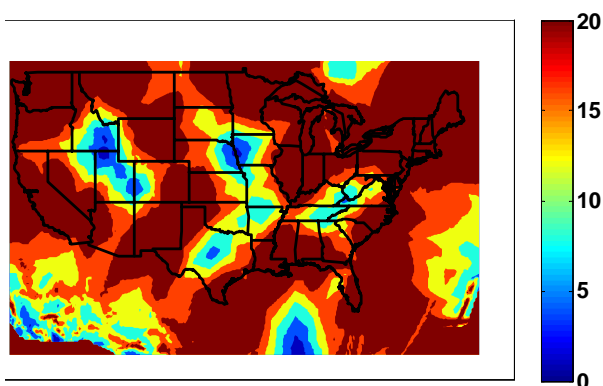

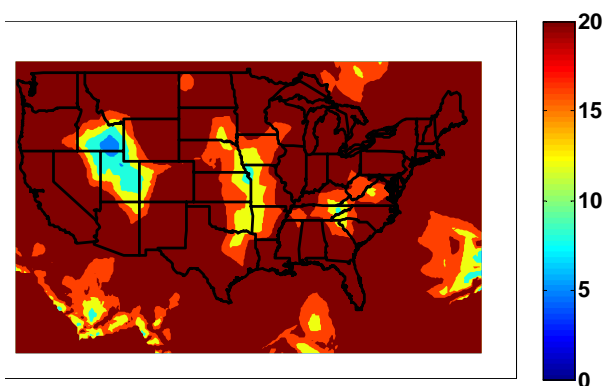**Figure 16: 9th pulse signal strength relative to the strongest cross-rate interferer, in dB.**
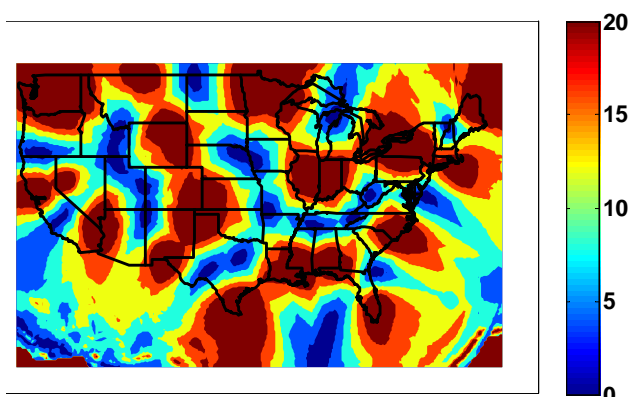
**Figure 17: 9th pulse signal strength relative to the second strongest cross-rate interferer, in dB.**

Figure 18: 9th pulse signal strength relative to the third strongest cross-rate interferer, in dB.

Figure 19: 9th pulse signal strength relative to the fourth strongest cross-rate interferer, in dB.

Worst case cross rate error performance occurs when the relative signal strength is close to zero, shown as blue in these plots. However, from these plots (especially Figure 19) it is evident that few areas within CONUS will see three or more interfering stations (of course, we have not yet taken into account skywave). Hence, a more accurate theoretical representation of cross rate percentages is shown in Figure 20, where high end estimates of 20%-25% are much closer to actual observed performance.
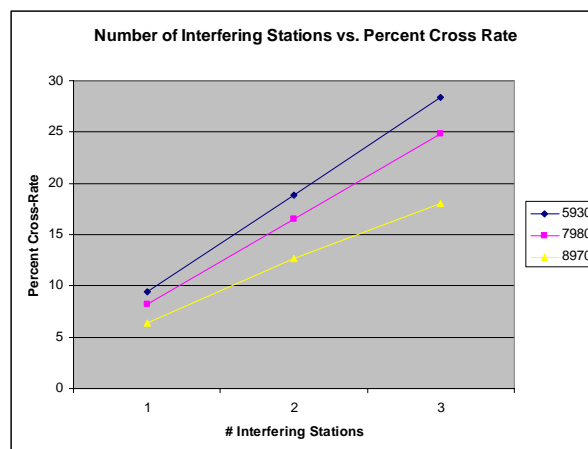
**Figure 20: Cross rate interference based on the number of interfering stations.**

DATA COLLECTION

A prototype Loran Data Capture system (LDaC) developed by Alion Science & Technology was used to capture the Loran data used in this study. A photograph of the system in operation appears as Figure 21, the software interface is shown in Figure 22.
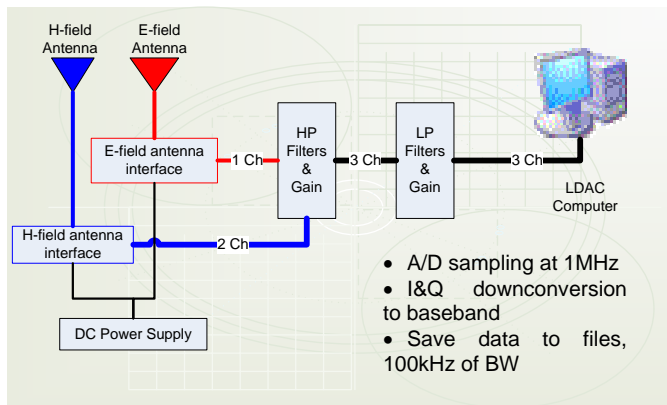
The LDaC system can capture Loran data using an H-field antenna (2 channels) and/or an E-field antenna (1-channel). The system is composed of the active antennas, a set of bandpass filters (8th order Bessel filters centered at 100kHz, with cutoffs of 50 and 150kHz) with programmable gain, and then the LDaC computer itself (see Figure 23). The LDaC computer samples the RF signal at 1MHz, using 12bits of resolution. The data is then I and Q (in-phase and quadrature) demodulated to baseband, digitally low-pass filtered, and decimated to 100 kHz.

Figure 21: LDaC system in operation.
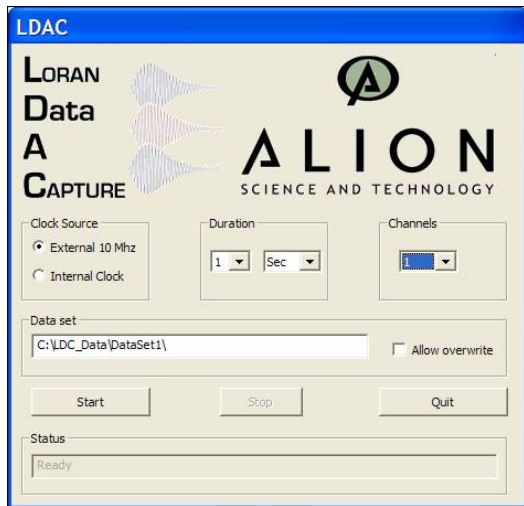
Figure 22: LDaC software graphical used interface.

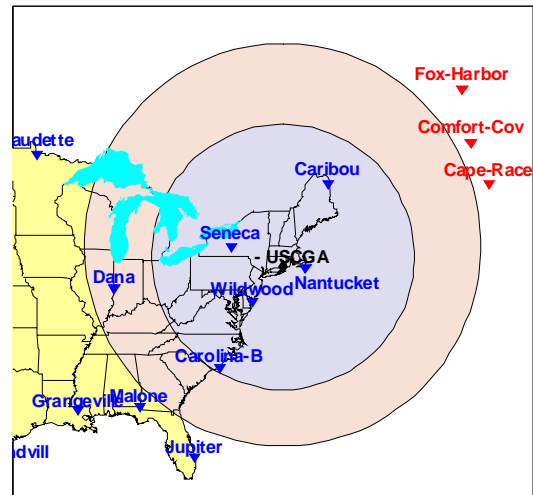**Figure 24: Loran stations visible from the USCG Academy.**
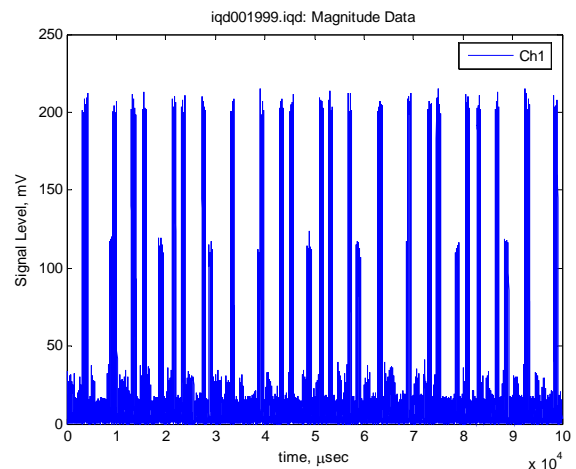

Figure 23: Block diagram of LDaC system.

The primary source of data for this research was collected at the US Coast Guard Academy (USCGA) in New London, CT. For this location, the closest Loran towers are shown in Figure 24; the strongest stations are Nantucket, Wildwood, Seneca, Carolina Beach, and Caribou, in that order.

A typical one second data set (magnitude only) is shown in Figure 25. Some of the aforementioned points that can be seen in this plot are the repetition of pulses at constant GRIs, as well as a dual-rated station which occurs on two rates. Additionally, the presence of noise makes it difficult to identify some of the stations which are farther away, but may still cause cross-rate events.
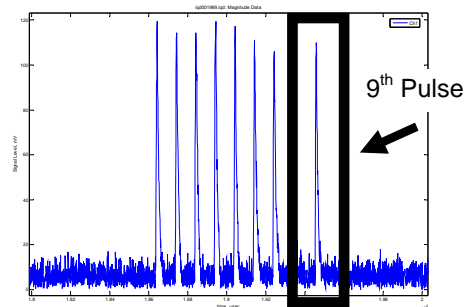
Looking closer at a group of pulses from the tower in Wildwood, NJ (see Figure 26), the 9th data pulse can be clearly seen.

Figure 25: One second of Loran data (magnitude only) sampled at 100 kHz.

Figure 26: Zooming into one GRI of data from Wildwood, NJ.

Figure 27 through Figure 30 show the average signal amplitude of every rate visible at USCGA. The chain (rate) with the most usable stations is the 9960 chain which is the Northeast United States (NEUS) Loran chain. The Loran Support Unit (LSU) in Wildwood was transmitting 9th pulse data during this collection at this rate. All of the stations that are visible in the other three chains are the second rates for the stations in the 9960 chain. Because each plot was averaged without accounting for the phase code changes between groups, only 4 of the 8 pulses are seen, with the exception of LSU, whose 9th pulse is seen but at a smaller magnitude due to the time shifts in modulation.
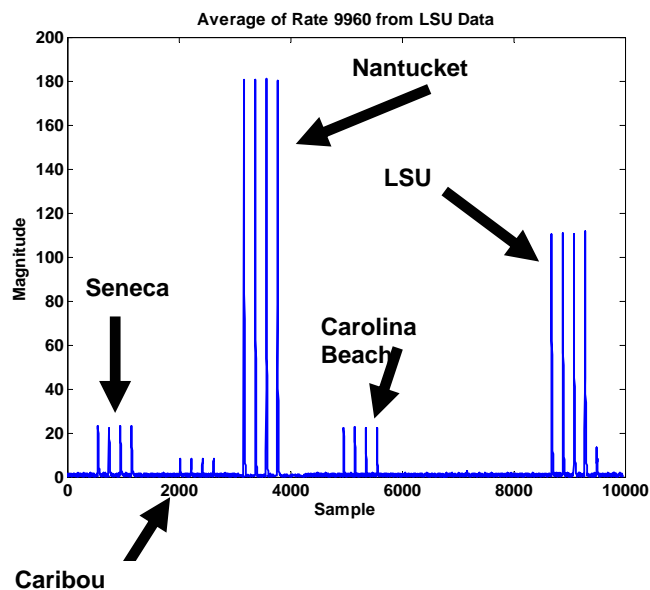

Figure 29: One GRI of the 7980 chain, averaged, showing relative signal magnitudes.
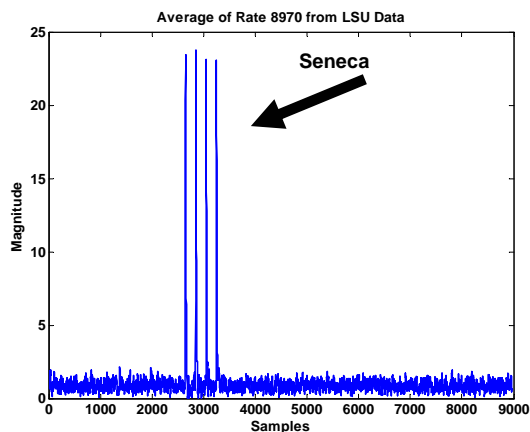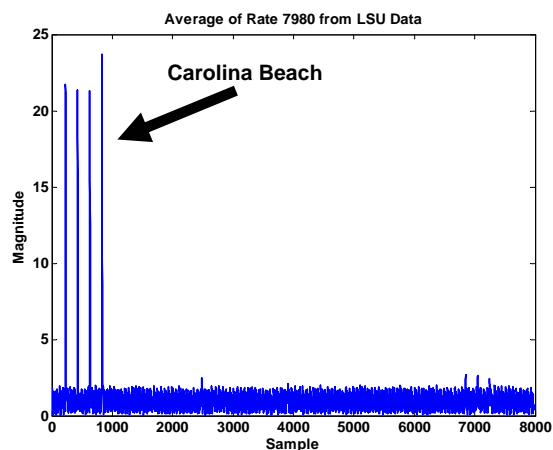

Figure 27: One GRI of the 9960 chain, averaged, showing relative signal magnitudes.
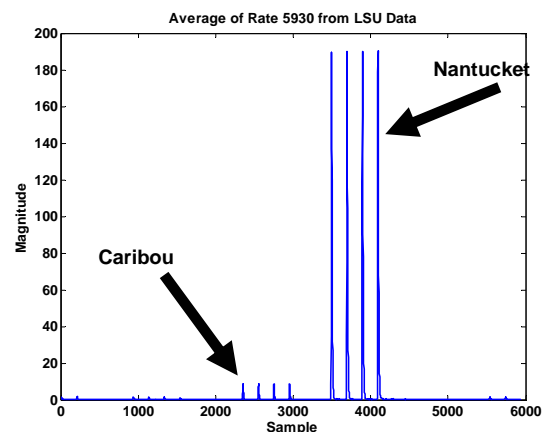

Figure 30: One GRI of the 5930 chain, averaged, showing relative signal magnitudes.

As discussed in prior sections, the relative strength between the 9th pulse signal and each possible interferer is crucial in determining the cross rate interference's contribution to symbol errors. Strong signals, arriving at the receiver from nearby transmitters, will have a much more significant affect on 9th pulse recognition than the weaker, farther away transmitters. In this particular area the station of greatest concern is Nantucket, broadcasting on 5930. A typical example of cross rate interference on 9960 is shown below in Figure 31. Note that the smaller interference from Caribou does not actually have any impact on the 9th pulse from LSU due to the lack of time overlap; however, Nantucket's first pulse does in fact interfere with the 9th pulse.
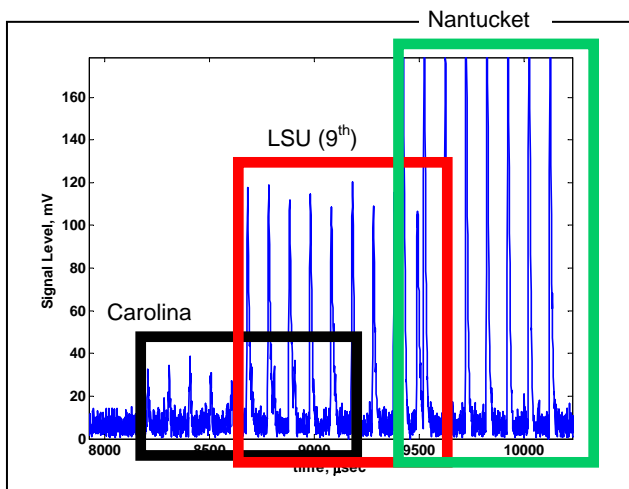

Figure 28: One GRI of the 8970 chain, averaged, showing relative signal magnitudes.

Figure 31: Cross-rate example.

$$\max_{k} \int r(t)\, s_k(t)\, dt$$

Therefore, to implement the 9th pulse receiver, the 32 lowpass equivalent signals can be used. Actually, since the 32 signals are purely time delays of each other (and the shapes of the lowpass equivalent signals seem identical except for the phase shifts), only one signal template is needed. This basic waveform could be estimated from the 8 unmodulated pulses in each group to account for an non-ideal characteristic of the modulator, antenna, and channel.

Figure 32: Received Loran pulse envelopes.

SIGNAL SPACE – REALITY

The error curves above are based upon the theoretical definition of the 9th pulse signals. To assess what happens in practice (since we know that the Loran transmitters and towers do not perfectly replicate the signals), we recorded several hours of 9th pulse transmissions from LSU at USCGA. Having knowledge of the ground truth during these transmissions, we sorted the recording by the signal transmitted, then averaged to observe the signals in space, at the receiver (we also deleted those pulses hit by cross rate interference, using the algorithm developed above, to improve the accuracy of these averages). The resulting envelopes are shown in Figure 32; we clearly observe both the coarse and fine time delays expected. While the average envelopes closely resemble the theoretical versions, the resulting phase of the carrier was somewhat different. Paralleling Figure 10, Figure 33 shows the lowpass equivalent signals (of one coarse group only) on the complex plane. While the phase separations of 45° are apparent, the lines are not radials out from and back into the origin (the circles are included to help align the results – in other words, the phase drift observed in the left hand plot matches up with the first 50 µsec of the pulse envelope). Our best estimate is that the phase drift is caused by the transmitter antenna not being precisely tuned to 100kHz.

The lowpass equivalent signals n Figure 33 are also useful for constructing a receiver for the 9th pulse modulation. A common receiver implementation, optimal if the channel is modeled as simply additive white Gaussian noise, is the matched filter or correlator receiver. If $r(t)$ is used to represent the received data and $s_k(t)$ is the kth possible signal, then this receiver decodes to that signal most closely matched (or is highly correlated with) the data
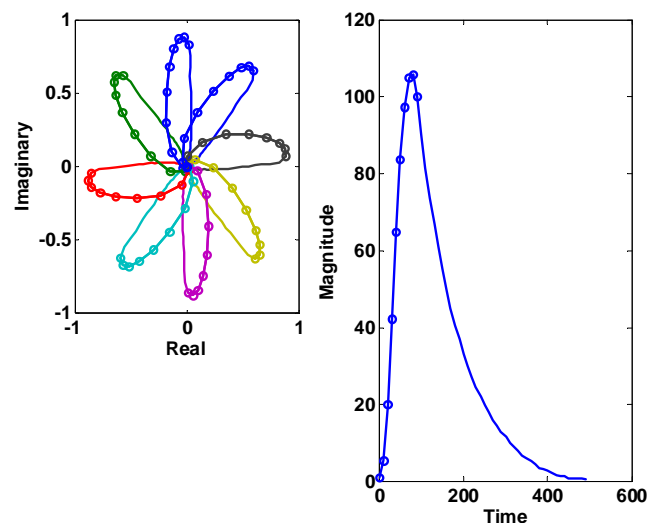

Figure 33: 9th pulse signals at the receiver: lowpass equivalent signal on the complex plane (one coarse group only) and the time domain envelope of one pulse. The circles help to align the two.

RESULTS

For this preliminary study, a limited amount of recorded data of LSU transmissions was available (LSU was transmitting 9th pulses on an experimental basis). Ultimately, 80,320 9th pulses (approximately two hours of data) were analyzed. Of those, our cross-rate algorithm tagged 24,370 pulses as being hit by cross rate interference. The remaining "clean" pulses were demodulated by a simple matched filter receiver with zero errors. This result is not surprising as the SNR for LSU at USCGA is approximately 22dB (at which we expect a symbol error rate of 10^{-5}). For such a small data set, zero measured errors is reasonable.

More interesting is our examination of the pulses that were affected by cross-rate. From our earlier discussion on the errors due to cross rate, it is expected that much of the cross-rate caused by distant stations will not contribute very much error. In fact, our results, tabulated below, show that if we tried to demodulate 9th pulses using a matched filter receiver, Nantucket was the only station whose cross rate interference contributed to symbol errors:

- Nantucket 5930 (5 dB higher) – 3230 of 7450 9th pulses were demodulated incorrectly

- Seneca 8970 (down ~15 dB) – 0 of 4372 9th pulses were demodulated incorrectly

- Carolina Beach 7980 (down ~15 dB) – 0 of 5673 9th pulses were demodulated incorrectly

- Caribou 5930 (down 20 dB) – 0 of 6876 9th pulses were demodulated incorrectly

It is also educational to examine the impact of individual cross rate hits on receiver performance. Figure 34 through Figure 36 provide insight into the effect of two hits from Nantucket (a strong interferer, stronger than LSU) and one from Seneca (a weak interferer). In each figure, the left subplot shows the lowpass equivalent signals on the complex plane; the right subplot shows the magnitude of the envelope of the received data. The color coding is green for truth of the transmission, red is the received data, and blue is the decoded result from the matched filter. The titles define the symbol numbers for the truth and decoded values, and show which station caused the interference. For example, Figure 34 shows one instance of a symbol error caused by interference from Nantucket. It is apparent that the interfering signal shifted the transmitted signal to the left in time, as well as causing a phase offset; these specifications matched more closely with a symbol 13, whereas a 29 was transmitted. Figure 35 shows one instance of interference from Nantucket that did not cause a symbol error. It is apparent that the interference occurred well after any of the 32 9th pulse

signals, and therefore did not have a detrimental impact on the output of the matched filter operation. Finally, Figure 36 shows that interference from a weaker station does not cause a symbol error. The interfering signal is so weak that it does not cause a demodulation error. In fact, it is difficult to see any impact on the received signal from the interference.
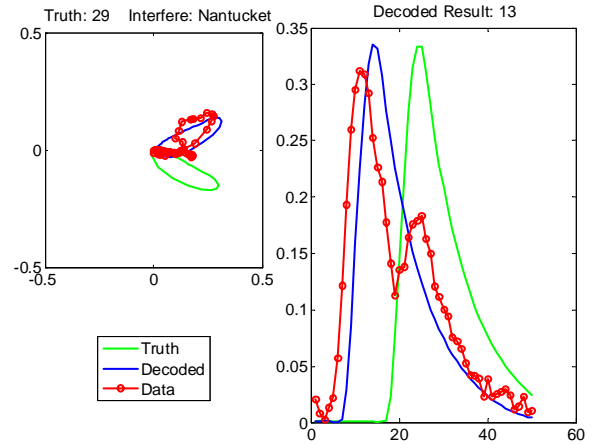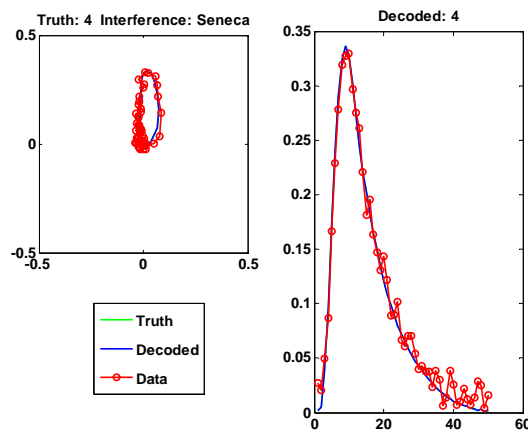

Figure 34: Cross-rate example: incorrectly decoded pulse due to cross-rate interference from Nantucket.
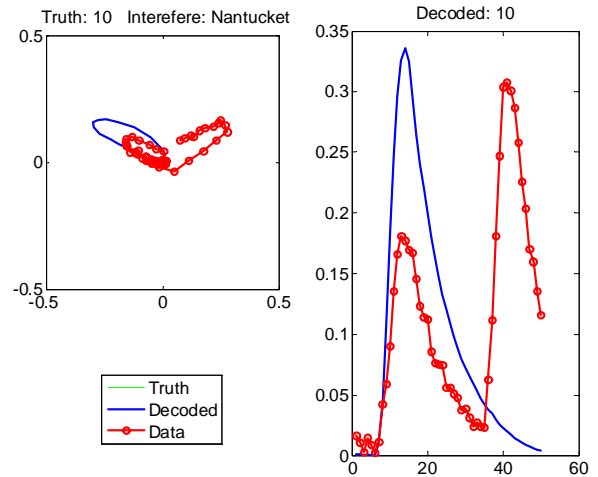
Figure 35: Cross-rate example: correctly decoded pulse in the presence of cross-rate interference from Nantucket.

Figure 36: Cross-rate example: correctly decoded pulse in the presence of weak cross-rate interference from Seneca.

CONCLUSIONS/FUTURE WORK

Our initial assessments from this research strongly support the theoretical expectations. Error probabilities are representative of those determined mathematically and the signal space model is reasonably matched by the observed signals in space. Understandably these conclusions are drawn from a relatively small data set. It is our intention to expand our analysis to longer data sets taken under various conditions.

While LSU only transmits 9th pulse data on an as-needed, experimental basis, Loran stations Jupiter and Seneca are currently transmitting 24/7. Late in 2005, we collected station Jupiter data in Charleston, SC. The location was selected so as to yield a SNR at the lower limit of what might be observed in CONUS; hence, we hope to use it to assess the symbol error rates due to channel noise alone. We are in the process of analyzing this data (it suffers from significant amounts of cross rate from two stronger stations, Carolina Beach and Malone). Additionally, as we collected data over a 24 hour period, we can look at the effect of skywave interference in the evening data. In the near future (Feb. 2006) we plan to collect station Seneca data in Ohio, a location affected more severely by both cross-rate interference and skywave.

In addition to data analysis, it is our goal to further explore the nature of cross rate interference with respect to 9th pulse communications, particularly, its periodicity and deterministic nature.

REFERENCES

[1] "Vulnerability Assessment of the Transportation Infrastructure Relying on the Global Positioning System," Volpe National Transportation Systems Center, U.S. Department of Transportation, Office of Ass't Sec for Transportation Policy, Boston, MA August 2001.

[2] "LORAN-C User Handbook," United States Coast Guard, Washington, DC COMDTPUB P16562.6, 1994.

[3] W. N. Dean, "Clarinet Pilgrim System," Magnavox Technical Report FWD73-243, September 1973.

[4] G. W. Offermans, A. W. Helwig, and D. Van Willigen, "The Eurofix Datalink Concept: Reliable Data Transmission Using Loran-C," *presented at 25th Annual Symposium, International Loran Association*, San Diego, CA, 3 - 7 November 1996.

[5] S. C. Lo and P. Enge, "Broadcasting Data from an SBAS Reference Network over using Loran," *presented at Annual Meeting, Institute of Navigation*, San Diego, CA, 26 - 28 June 2000.

[6] B. Peterson, K. Dykstra, P. Swaszek, and J. M. Boyer, "High Speed LORAN-C Data Communications - June 2001 Update," *presented at Annual Meeting, Institute of Navigation*, Albuquerque, NM, 11-13 June 2001.

[7] B. Peterson, K. Dykstra, P. Swaszek, J. M. Boyer, K. M. Carroll, and M. Narins, "High Speed Loran-C Data Communications - Flight Test Results," *presented at Institute of Navigation (ION) GPS Conference*, Salt Lake City, UT, 11-14 September 2001.

[8] B. B. Peterson, K. Dykstra, P. Swaszek, J. Boyer, K. Carroll, and M. Narins, "Wagging the Tail & Flying with Loran-C Data Communications," *presented at 30th Annual Convention and Technical Symposium, International Loran Association*, Paris, France, October 2001.

[9] B. B. Peterson, A. Hawes, and K. Shmihluk, "Loran Data Channel Communications using 9th Pulse Modulation (ver 1.0)," Loran Support Unit, 2 Jan 2006.